
This is an electronic reprint of the original article.
This reprint may differ from the original in pagination and typographic detail.

Jalkanen, Jari; Trushin, Oleg; Granato, E.; Ying, See Chen; Ala-Nissila, Tapio
Equilibrium shape and dislocation nucleation in strained epitaxial nanoislands.

Published in:
Physical Review B

DOI:
[10.1103/PhysRevB.72.081403](https://doi.org/10.1103/PhysRevB.72.081403)

Published: 01/01/2005

Document Version
Publisher's PDF, also known as Version of record

Please cite the original version:
Jalkanen, J., Trushin, O., Granato, E., Ying, S. C., & Ala-Nissila, T. (2005). Equilibrium shape and dislocation nucleation in strained epitaxial nanoislands. *Physical Review B*, 72(8), 1-4. [081403].
<https://doi.org/10.1103/PhysRevB.72.081403>

This material is protected by copyright and other intellectual property rights, and duplication or sale of all or part of any of the repository collections is not permitted, except that material may be duplicated by you for your research use or educational purposes in electronic or print form. You must obtain permission for any other use. Electronic or print copies may not be offered, whether for sale or otherwise to anyone who is not an authorised user.

Equilibrium shape and dislocation nucleation in strained epitaxial nanoislands

J. Jalkanen,¹ O. Trushin,² E. Granato,³ S. C. Ying,⁴ and T. Ala-Nissila^{1,4}

¹Laboratory of Physics, P.O. Box 1100, Helsinki University of Technology, FIN-02015 HUT, Espoo, Finland

²Institute of Microelectronics and Informatics, Academy of Sciences of Russia, Yaroslavl 150007, Russia

³Laboratório Associado de Sensores e Materiais, Instituto Nacional de Pesquisas Espaciais,
12245-970 São José dos Campos, SP Brasil

⁴Department of Physics, P.O. Box 1843, Brown University, Providence, Rhode Island 02912-1843, USA

(Received 22 June 2005; published 12 August 2005; corrected 22 August 2005)

We study numerically the equilibrium shapes, shape transitions, and dislocation nucleation of small strained epitaxial islands with a two-dimensional atomistic model, using simple interatomic pair potentials. We first map out the phase diagram for the equilibrium island shapes as a function of island size (up to $N=105$ atoms) and lattice misfit with the substrate, and show that nanoscopic islands have four generic equilibrium shapes, in contrast with predictions from the continuum theory of elasticity. For increasing substrate-adsorbate attraction, we find islands that form on top of a finite wetting layer as observed in Stranski-Krastanow growth. We also investigate energy barriers and transition paths for transitions between different shapes of the islands and for dislocation nucleation in initially coherent islands. In particular, we find that dislocations nucleate spontaneously at the edges of the adsorbate-substrate interface above a critical size or lattice misfit.

DOI: 10.1103/PhysRevB.72.081403

PACS number(s): 81.10.Aj, 68.35.Gy, 68.65.-k

The shape and size of islands resulting from a growth process has been the subject of intense experimental and theoretical studies.¹⁻¹¹ There are still uncertainties as to whether the observed shape and size of islands correspond to a thermodynamic equilibrium state of minimum free energy, or whether they are limited by kinetic effects. In an equilibrium theory, the optimal size and shape result from a delicate balance of energy lowering through strain relaxation and energy cost through extra surface energy. Earlier works on equilibrium shape of coherent islands have used simple predefined faceted shapes in analytical calculations based on continuum elasticity theory.^{2,3} The resulting equilibrium shapes of two-dimensional (2D) islands can be classified according to the relative abundance of two types of facets, namely shallow and steep facets only. The role of possible wetting films has also been recently considered for the three-dimensional (3D) system of InAs on GaAs(001) (Ref. 4). However, in addition to assuming predefined shapes, in all these studies the role of possible dislocations in the islands has not been included.

In this work, we use an atomistic model to numerically study the equilibrium shape of strained islands allowing for both elastic and plastic strain relaxation without assumptions on predefined shapes. We adopt a 2D model here, but extension to more realistic 3D systems is also possible. The reduced dimension allows us to study all possible configurations within feasible computer time. Most of our results here are for relatively small, nanoscopic islands up to a few hundred atoms in size to examine deviations from the continuum theory of elasticity. In addition, we want to investigate the role of dislocation nucleation in determining the equilibrium shape and size of these islands. In an earlier approach, elastic and plastic strain relaxation have also been treated with a common formalism using vertically coupled Frenkel-Kontorova layers of finite length,⁵ where only particle displacements parallel to the substrate are allowed. However, such a model does not provide a realistic description of dislocation nucleation, whereas in our study, disloca-

tions of arbitrary type are allowed in the final equilibrium configuration.

In the 2D model we use for the strained adsorbate island and substrate the atomic layers are confined to a plane. Interactions between atoms in the system are described by a generalized Lennard-Jones (LJ) pair potential¹² $U(r)$, modified^{13,14} to ensure that the potential and its first derivative vanish at a predetermined cutoff distance r_c , given by

$$U(r) = V(r), \quad r \leq r_0;$$

$$U(r) = V(r) \left[3 \left(\frac{r_c - r}{r_c - r_0} \right)^2 - 2 \left(\frac{r_c - r}{r_c - r_0} \right)^3 \right], \quad r > r_0, \quad (1)$$

where

$$V_{ab}(r) = \varepsilon_{ab} \left[\frac{m}{n-m} \left(\frac{r_0}{r} \right)^n - \frac{n}{n-m} \left(\frac{r_0}{r} \right)^m \right]. \quad (2)$$

Here, r is the interatomic distance, ε_{ab} the dissociation energy, which can be different for substrate-substrate (ab=ss), adsorbate-adsorbate (ab=ff), and adsorbate-substrate (ab=fs) interactions, and r_0 is the equilibrium distance between the atoms. For $n=6$ and $m=12$, $U(r)$ reduces to the standard 6-12 LJ potential with a smooth cutoff. For most of the calculations we have chosen the values $n=5$ and $m=8$. In contrast to the 6-12 potential, this has a slower falloff. When combined with the variation of the cutoff radius r_c , this choice allows us to study the effect of the range of the potential. The equilibrium interatomic distance r_0 was set to values $r_{ss}=r_0$, r_{ff} , and r_{fs} for the substrate-substrate, adsorbate-adsorbate, and adsorbate-substrate interactions, respectively. The parameter r_{fs} for the adsorbate-substrate interaction was simply set as the average of the film and substrate lattice constants, i.e., $r_{fs}=(r_{ff}+r_{ss})/2$. The lattice misfit f between the adsorbate and the substrate can thus be defined as

$$f = (r_{\text{ff}} - r_{\text{ss}})/r_{\text{ss}}. \quad (3)$$

A positive mismatch $f > 0$ corresponds to compressive strain and negative $f < 0$ to tensile strain when the adsorbate island is coherent with the substrate. Calculations were performed with periodic boundary conditions for the substrate in the direction parallel to the adsorbate-substrate interface. In the calculations, the two bottom layers of the five-layer substrate were held fixed to simulate a semi-infinite substrate while all other layers were free to move. We checked that increasing the substrate thickness did not affect the results. Typically, each layer of the substrate contained about 100–500 atoms.

To obtain the equilibrium shape of the island for a fixed total number N of atoms without assuming any predetermined shapes, we use a systematic search approach. Each initial coherent configuration is described by a set of integer numbers, n_i , specifying the number of atoms in successive layers of the island. In terms of these quantities, the two types of facets, considered in the previous works,^{2,3} correspond to $n_i - n_{i+1} = 1$ for steep facets and $n_i - n_{i+1} = 3$ for shallow facets. The only physical restriction we impose is that the island has a reflection symmetry about a line through the center and overhangs are not allowed. Then, for each initial configuration, molecular-dynamics (MD) cooling was run to allow the system to relax and reach a minimum-energy configuration. The equilibrium shape for a given N is identified as the relaxed configuration with lowest energy among all the possible configurations. In the present case, this leads to complete relaxation of the interlayer bonds in the islands, while intralayer bonds remain strained.

First, we present the results where the potential parameters were chosen to be $\epsilon_{\text{ss}} = \epsilon_{\text{ff}} = \epsilon_{\text{fs}} = 3\,410.1$ eV and $r_0 = 2.5478$ Å corresponding to Cu substrate.¹² Phase diagrams for the equilibrium shapes as a function of total number of island atoms N and lattice misfit f are shown in Fig. 1(a), for two different cutoff radii $r_c = 3.82$ and 5.3 Å, which we call here the SR and LR cases, respectively. Different phases are labeled by the total number of layers in the island. In agreement with previous works,¹ there is a transition from a single-layer configuration (uniform flat wetting layer) to an island configuration, above a critical size or lattice misfit. However, unlike the results from continuum elasticity theory, the phase diagram is not symmetric with respect to the misfit parameter and thus the behavior for compressive and tensile strained layers is quite different. The asymmetry is more pronounced for the LR interaction potential, which includes significant contribution from next-nearest-neighbor atoms.

The predominant shapes of the islands in the phase diagram are shown in Fig. 1(b). We performed a systematic classification of these shapes for $1 \leq N \leq 105$ and $-10\% \leq f \leq 10\%$. The strained film remains flat roughly between $-5\% \leq f \leq 5\%$ (SR) and $-3\% \leq f \leq 7\%$ (LR, up to $N = 63$). The region of 2D islands appears already for $N = 11$ for the largest misfits, and the extent of the flat film regime in the f - N plane shrinks for increasing N [cf. Fig. 1(a)]. The shapes A, C, and D alternate with N , with the shapes A and C being most common while B is relatively rare.

The critical size along the transition line from single-layer to finite height island shape in our phase diagram can be

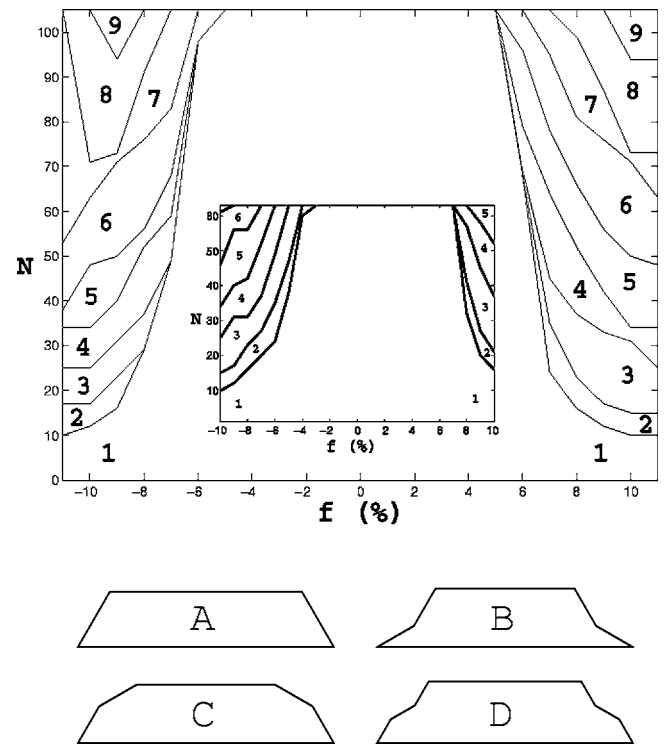


FIG. 1. Phase diagram showing island height as a function of number of atoms N and the lattice misfit f for the SR (main figure) and LR (inset) potentials. Different phases are labeled by the number of layers in the island. Predominant island shapes in the phase diagram for nanoscopic islands. Shape D is not predicted by continuum elasticity theory here.

fitted to a power law as $N_c \propto f^{-a}$, with $a \approx 3.8$, consistent with the result from the continuum elasticity approach.² Similar behavior has also been found in a model of vertically coupled Frenkel-Kontorova chains.⁵ For the SR potential, a rough estimate through simple bond counting yields a value for the ratio of the shallow to steep facet surface energies $r \approx 0.5$. According to Ref. 2, this would imply an equilibrium shape of only either the steep facet with truncated top or steep facet followed by shallow facet and then truncated top, corresponding to the shapes A and C in Fig. 1(b). Although these general features agree with the elastic model calculations, there are important differences. First, there is compressive-tensile asymmetry in the shapes which is particularly pronounced for the LR potential. In addition, for small islands (less than about 200 atoms) there are additional equilibrium shapes B and D in regions of the phase diagram in Fig. 1(a) that were not accounted for in Ref. 2. More recent work based on the elasticity theory³ finds that the possibility of shallow facets below the steep ones, as observed in shape B, should also be considered. However, shape D that we find here remains unaccounted for by the continuum elasticity theory.

If the number of atoms N is sufficiently large, then the optimal size and shape for the island depend on the subtle balance between the strain energy, the surface energy of the island, and the interface energy between the island and the substrate. Depending on the parameters of the interatomic potentials, phases other than those shown in Fig. 1(a) can

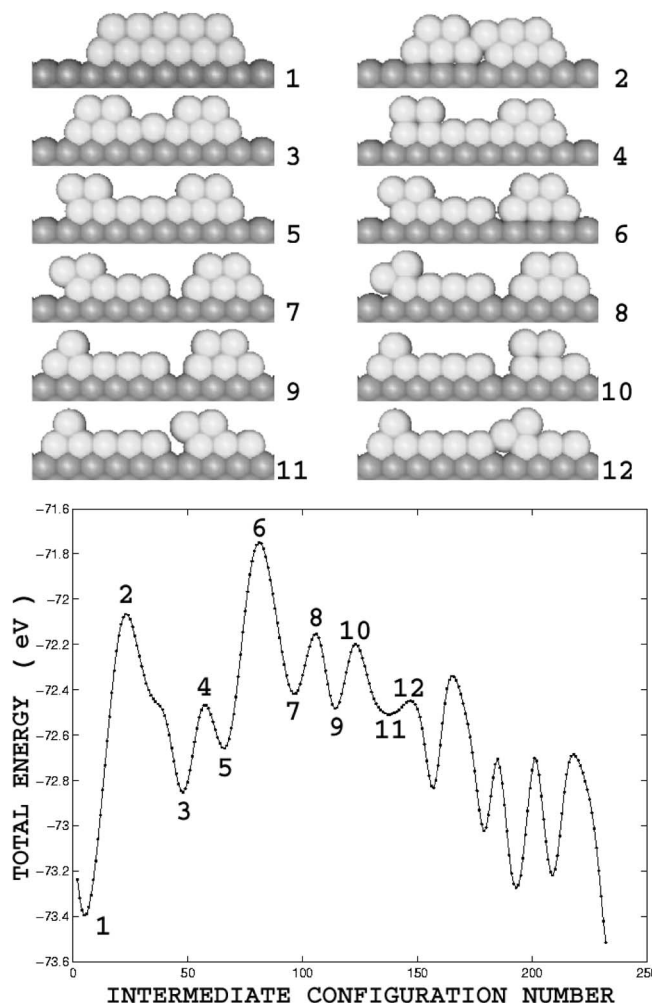


FIG. 2. First 12 particle configurations (upper frame) corresponding to the labeled extrema in the energy profile (lower frame). This minimum-energy path has been generated by NEB and it corresponds to the shape transition boundary for an 11-atom island to a flat layer. The final flat configuration (not shown here) is reached so that the remaining two second-layer atoms in configuration 12 move close to the island edges and descend to the substrate.

occur. We consider here the situation where $\epsilon_{fs} > \epsilon_{ss} = \epsilon_{ff}$. For small misfit, complete wetting occurs, as expected. However, at large enough misfit, e.g., $f=8\%$ and for $\epsilon_{fs}/\epsilon_{ss} \approx 1.5$, the behavior is totally different. In this case, for a system of lateral size 200 and for total number of atoms $N=600$, the minimum-energy configuration corresponds to that of a wetting layer with an island of shape A with 26 layers high on top of it. This result also implies the existence of an optimal size for a given shape of the island. Our results thus correspond to the 2D version of the 3D islands in Ref. 4. Thus by varying the misfit and the substrate-adsorbate interactions, we find configurations corresponding to the commonly known different modes of adsorbate growth (Frank-Van der Merve, Stranski-Krastanow, and Volmer-Weber), which occur as minimum-energy configurations in our model. Detailed results for the different regimes will be published elsewhere.¹⁵

We have also studied minimal-energy paths for transitions

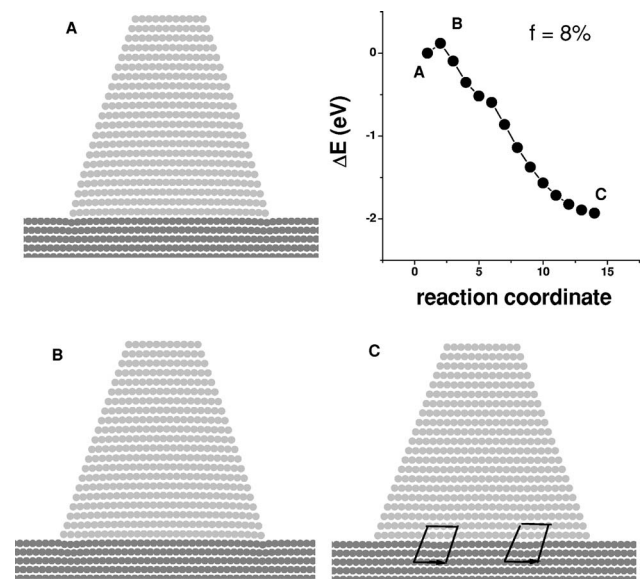


FIG. 3. NEB minimum energy profile and particle configurations for a 411-atom strained island, where a pair of dislocations nucleate at the edges of the island. Closed paths in (c) are the Burgers circuits around the dislocation cores in the final state. See text for details.

from a flat layer to an island of finite height. For a fixed number of atoms N and misfit f close to the transition, we consider two shapes corresponding to the different states across a transition line from 1 to 2 ML in Fig. 1. Given these as initial and final states, we use the nudged elastic band (NEB) (Ref. 16) method to generate a (locally) minimum-energy transition path between these two different shapes. We follow the similar approach used in the study of defect nucleation in strained epitaxial films introduced recently.¹⁴ As an initial guess for the transition path we use a simple linear interpolation. The resulting energy profile and configurations along the minimum-energy path are shown in Fig. 2. As it is clear from the figure, there is a large energy barrier separating the two distinct minima corresponding to the two different shapes. This is generally true for any two states bordering the transition line in our phase diagram in Fig. 1. Thus, depending on the time scale, the transition may occur too slowly to be observed during epitaxial growth. The existence of this large energy barrier, obtained with our atomistic model, supports the conclusion from the elastic theory calculations^{2,3} that the transition can be regarded as first order.

For sufficiently large islands or misfits we find that relaxing an initial configuration with MD cooling already generates dislocations in the lowest-energy state. This implies that the energy barrier for dislocation nucleation is zero or negligible above a critical value. We find that the dislocations nucleate from the edges of the adsorbate-substrate interface for an initially dislocation-free island. This is in contrast with the mechanism for a flat uniform film,¹⁴ where dislocations nucleate from the top layer. This result provides strong support from atomistic calculations for the conclusions obtained within continuum elasticity theory.^{6,7} To better understand the dislocation nucleation mechanism, we consider a region

of phase space where the dislocation is not necessarily spontaneously generated, i.e., there may exist a finite barrier for nucleation. The transition path for dislocation nucleation is generated using the NEB approach with the coherent island and the island with dislocation as the initial and final states. As an initial guess for the transition path we use again a simple linear interpolation scheme between the coherent and incoherent states. The resulting energy profile and configurations along the minimum-energy path found are shown in Fig. 3. The sequence of configurations along the transition path shows that the two dislocations nucleate successively at the separate edges of the island and then propagate inwards. The energy barrier for a fixed island size decreases with misfit. This is consistent with experimental results,¹⁰ which show that small islands are dislocation-free but dislocations appear in the island when it reaches a critical size.

In summary, we have studied the equilibrium shapes, shape transitions, and strain relaxation processes of strained, nanoscopic epitaxial islands. The equilibrium shapes are de-

termined via energy minimization for different shapes without any preassumptions about the possible shapes, and they differ considerably from the elastic continuum predictions. The systematic transition path search combined with the NEB approach allow us to determine the energy barrier and transition path for the shape transition and for dislocation nucleation in initially coherent islands. In particular, we find that dislocations can nucleate spontaneously at the edges of the adsorbate-substrate interface above a critical size or misfit. Although these calculations were performed for a 2D atomistic model, the method can also be extended to more realistic 3D systems.

We wish to thank Professor Joachim Krug for useful discussions. This work has been supported in part by Fundação de Amparo à Pesquisa do Estado de São Paulo—FAPESP (Grant No. 03/00541-0) (E.G.) and the Academy of Finland through its Center of Excellence program (T.A-N., J.J., and O.T.).

¹P. Politi, G. Grenet, A. Marty, A. Ponchet, and J. Villain, *Phys. Rep.* **324**, 271 (2000).

²I. Daruka, J. Tersoff, and A.-L. Bara'bási, *Phys. Rev. Lett.* **82**, 2753 (1999).

³I. Daruka and J. Tersoff, *Phys. Rev. B* **66**, 132104 (2002).

⁴L. G. Wang, P. Kratzer, N. Moll, and M. Scheffler, *Phys. Rev. B* **62**, 1897 (2000).

⁵C. Ratsch and A. Zangwill, *Surf. Sci.* **293**, 123 (1993).

⁶H. T. Johnson and L. B. Freund, *J. Appl. Phys.* **81**, 6081 (1997).

⁷B. J. Spencer and J. Tersoff, *Phys. Rev. B* **63**, 205424 (2001).

⁸J. Tersoff and F. K. LeGoues, *Phys. Rev. Lett.* **72**, 3570 (1994).

⁹R. A. Budiman and H. E. Ruda, *J. Appl. Phys.* **88**, 4586 (2000).

¹⁰A. Ponchet, A. Le Corre, H. L'Haridon, B. Lambert, S. Salan, D.

Alquier, D. Lacombe, and L. Durand, *Appl. Surf. Sci.* **123**, 751 (1998).

¹¹H. Uemura, M. Uwaha, and Y. Saito, *J. Phys. Soc. Jpn.* **71**, 1296 (2002).

¹²S. Zhen and G. J. Davies, *Phys. Status Solidi A* **78**, 595 (1983).

¹³O. Trushin, E. Granato, S.-C. Ying, P. Salo, and T. Ala-Nissila, *Phys. Status Solidi B* **232**, 100 (2002).

¹⁴O. Trushin, E. Granato, S.-C. Ying, P. Salo, and T. Ala-Nissila, *Phys. Rev. B* **65**, 241408(R) (2002); **68**, 155413 (2003).

¹⁵J. Jalkanen *et al.*, (unpublished).

¹⁶H. Jónsson, G. Mills, and K. W. Jacobsen, in *Classical and Quantum Dynamics in Condensed Phase Simulations* edited by B. J. Berne *et al.* (World Scientific, Singapore, 1998).